Increasing Efficiency and Reliability of RF Machinery Testing Using Cartesian Robotics and Automatic Data Collection

Paul Miller, Sam Baliki, Rami Hanna, James McCusker, and Brian C. Wadell

***Abstract*—When analyzing high-throughput radio frequency (RF) chip testing machinery, the limitations of manual tests are evident. Manual testing can be imprecise and costly. Robotic automation, force feedback, and remote access can be used as comprehensive solutions that modernize testing procedures. The integration of a Cartesian robot with an automatic tool-changer brings precision and repeatability to testing processes without the need for an operator. Furthermore, the addition of a camera and constant load monitoring allows for imaging and fault detection. These features address the complications posed by delicate and expensive RF coaxial connectors. Most importantly, this system enables efficient data collection that lays the foundation for future research and process characterization.**

***Keywords*— Automation Systems, Mechatronics Systems, Mechanism Design**

I. Introduction

As high frequency chipsets become increasingly common, the coaxial cables needed to carry such signals have drastically decreased in size. RF chip testing machines are used to test millions of computer chips per week. However, running and testing these machines requires the repetitive mating of miniature RF coaxial connectors. These cables are delicate, costly, and their small size demands tight tolerances. The handling of these connectors is typically performed manually, which can easily lead to damaged or broken cables due to human error. As added protection, cables can be compliant in one or more degrees of freedom to help prevent accidental damage. The cables used in this paper have a spring beneath the female connector to achieve this compliance. The proposed Cartesian robot system will automate this process to prevent damage and increase the capabilities of RF testing.

This system is designed using kinematics similar to today's common 3D printers. Usage of such mechanisms has increased over time with growing standards to improve robot reliability and quality [1]. Using robotics, the RF cable mating process is more reliable and more easily automated. While manual processes necessitate on-site work, especially when several handheld tools are being used, automation allows technicians to run tests remotely and set autonomous testing procedures to run in the background. To fully automate this process, a tool-changer can be used to switch between the desired tools.

A robotic solution also creates the framework for a more intelligent system. The inclusion of sensors allows the robot to gather data, which can be used to further increase its functionality. The suggested platform includes a force sensor and a camera. The force sensor can be used to generate force curves during cable mates, producing better characterization of a given interaction between a male and female plug. This can be used to detect faults during plugging and stop the test before damaging any components. The camera sensor can be used to take pictures of the connectors before and after mates, as well as when a fault is detected by the load cell. This can be used to build a database for training a machine learning algorithm. In the future, this algorithm could be used to determine the location of connectors in the X-Y plane and detect damaged connectors for removal.

Importantly, this system has been developed in collaboration with Teradyne Inc, whose semiconductor test platform serves as a cornerstone for designing and testing this system. Pictured in Figure 1 is the plug arrangement commonly used on the semiconductor test machines. The cable fixture serves as a common mounting plate for the cables used at Teradyne Inc. The plugs are numbered clockwise, starting from the datum plug.

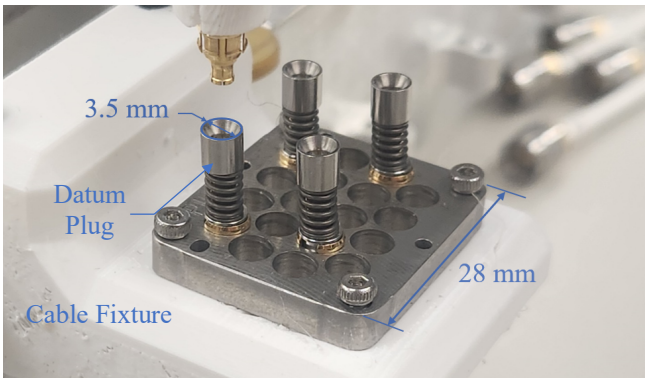

Figure 1: Cable Fixture and Plug Reference

II. Background

A. Impact of Automation on Industry

Automation has become a crucial aspect of modern industrial spaces, and this automation can be extended to RF machinery testing. In 2006, seven large European manufacturing companies were surveyed about how automation could be beneficial, to which the following results were concluded: "Automation will give cost savings within production (100%), give possibilities for higher efficiency (98%), increased competitiveness (97%), and productivity (94%) … Many respondents also acknowledged that the main benefit of automation is that it enables production with a minimum of employees (85%)" [2]. This study shows a trend in many industries towards automation. Additionally, there is a need to reduce the cost of a technician servicing these machines.

*Sam Baliki, Rami Hanna, Paul Miller (Correspondence Author, millerpcm@gmail.com), and James McCusker are with Wentworth Institute of Technology [Boston, MA 02115]; Brian Wadell is with Teradyne Inc [North Reading, MA, 01864].

This is possible with an automated system that provides remote access to the machine, and control of different data acquisition devices via a tool-changer.

B. Current State of the Art

The current state of automatic cable mating and automatic RF testing lacks many of the features this solution offers. The RF testing processes "in most of the semiconductor fabrication industries is either fully manual or employs expensive test systems" [3]. Other similar systems typically focus on the orientation of the plugs, and do not incorporate force feedback for damage detection [4]. Since this project holds the cables coaxially, only the position of the cable is relevant to the successful mate of a cable.

A central aspect of this system involves the acquisition of force data on the end effector. Currently, there is little information available on the mating force of RF connectors used in industry. Samtec has generated force curves during the mating and un-mating of their own connectors through empirical testing and finite element analysis (FEA) simulation [5]. These simulations model the deflection of the contacts and the friction force inherent in male-female connector interaction during a mate (Figure 2). Similar data is not currently available for RF connectors used in industry. A platform that can collect this data not only allows for real time fault detection, but additionally supports further analysis regarding the characteristics of RF cable mating curves.

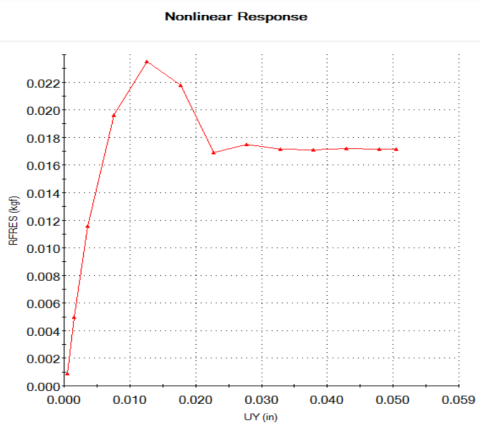

Figure 2: Samtec Mating FEA Mating Curve [5]

Huang [6] developed a robotic wire harness system capable of similar force-based fault detection. However, this platform did not manipulate delicate RF connectors, and used an expensive robotic arm rather than a cartesian gantry. Figure 3 displays mate regions of the connectors used in [6], demonstrating how a force curve can be utilized to detect faults during automatic cable mating processes.

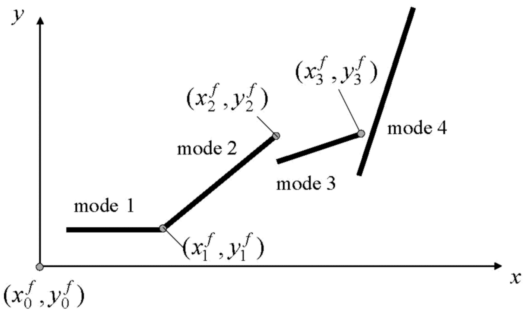

Figure 3: Piecewise Model of Mating Process [6]

III. System Design

A. Gantry Design

To determine the level of accuracy necessary, a tolerance analysis was performed on one of the smaller connectors commonly used in industry: the Sub Miniature Push-on Micro (SMPM) connector. The coaxial tolerance needs to be within ± 0.18 millimeters in the worst case to successfully mate (Figure 4). With 2 millimeter pitch lead screws and 1.8 degree stepper motors, a theoretical resolution of 0.625 micrometers is possible via micro-stepping. However, testing has shown a repeatability of around 0.01 millimeters, which is more than sufficient for the tolerance analysis performed.

To attain precise and repeatable linear motion, the gantry design utilizes common components such as leadscrews, NEMA 17 stepper motors, and linear rails. These components were selected for their balance of high resolution and cost-effectiveness. To address the concern of backlash, anti-backlash nuts have been implemented on each lead screw. Figure 5 shows these design principles implemented on the robot.

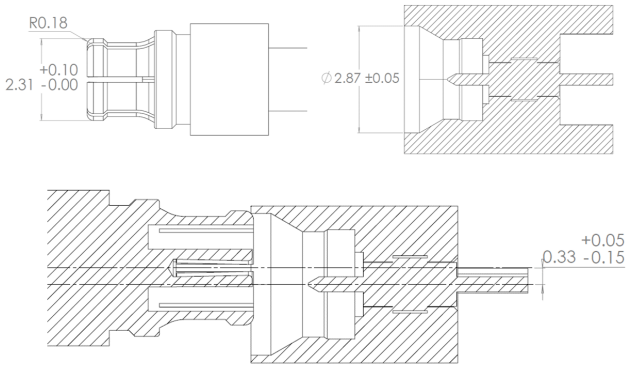

Figure 4: SMPM Tolerance Analysis

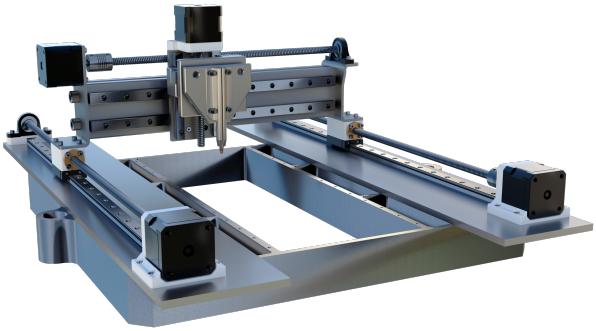

Figure 5: Render of Robot

To determine the necessary size of the X-axis, SOLIDWORKS simulations were run to determine the amount of deflection that would occur under expected loads at the end effector. The maximum plug force and maximum distance from the axis were used to calculate an expected moment of 4 Newton-meters, which was applied in the simulation. With the 30 millimeters by 60 millimeters support used, the absolute deflection was determined to be no more than 0.1 millimeters, of which the horizontal component of this deflection would be 3×10^{-5} millimeters (Figure 6). This deflection is negligible for the system's applications.

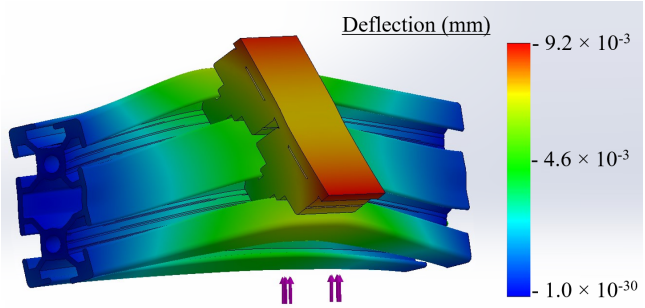

Figure 6: Aluminum Deflection Analysis

B. *Z-axis Assembly*

The Z-axis uses a 1.8 degree stepper motor with a 2 millimeter pitch lead screw built into the motor to allow for maximum travel distance. From the Z-axis, a tool-changer is mounted via a 10 kilogram load cell. The load cell is positioned to continuously monitor the force, regardless of the active tool. During this process, the signal from the load cell is fed through an HX711 amplifier into a Raspberry Pi 4 B to store the data and provide real-time feedback.

C. *Tool-Changer Design*

Testing RF chips often involves the use of various tools. To ensure fully automatic capability, a tool-changer is used to swap between different toolheads without the need for a technician. While a cable toolhead is currently the sole tool being used, this platform is designed to be an expandable high-precision test fixture. A structural interface is required to construct a repeatable mechanical connection that allows for routine attachment and detachment while bearing load [7].

A kinematic coupling is a type of structural interface that adheres to exact constraint design. This means that the number of contact points between the two bodies exactly equals the degrees of freedom that are constrained. Therefore, six contact points are needed to fully constrain all six degrees of freedom of a part (considering three translations along its orthogonal axes and three rotations about its orthogonal axes). In other words, kinematic couplings are statically deterministic, creating a structure that is theoretically impossible to undergo internal stresses. This avoids a multitude of design issues: internal strain can lead to part misalignment; unintended elastic potential energy can be released unexpectedly, harming system performance; and over-constrained parts can settle into indeterminate positions [8]. A kinematic coupling therefore serves as an effective apparatus for a tool-changer mechanism.

While a variety of kinematic coupling types exist, one traditional version is the Maxwell-style coupling. This interface consists of three spherical surfaces corresponding to three V-grooves, all oriented towards a central point in a triangular formation. As seen in Figure 7, this central point should be the intersection of the angle bisectors for maximum stability and repeatability. This optimizes the layout geometry such that rotation about a given ball-to-ball axis' instantaneous center is maximally resisted by the third ball-grove pairing. Any triangular configuration can be used, however using an equilateral triangle layout is a simple technique to establish the optimal central point as it causes this intersection point to coincide with the coupling centroid [7].

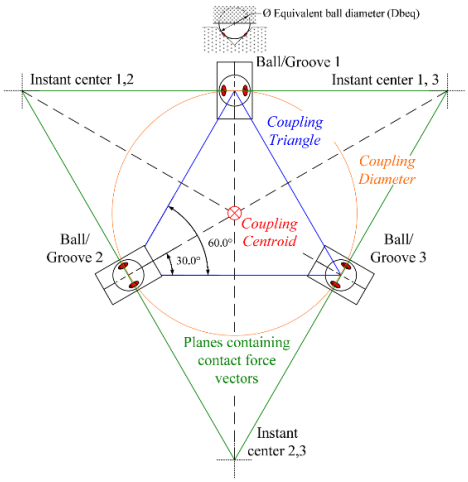

Figure 7: Maxwell Kinematic Coupling Diagram [7]Preload force is another critical aspect of kinematic couplings. To hold the two bodies together, a preload force must be applied to establish initial stiffness. The magnitude of this force must be relatively high while avoiding material deformation. In heavy-duty applications, this preload may be provided through a series of bolts and compressed springs. For lightly loaded systems, a magnetic preload may provide sufficient force to guarantee adequate stiffness [9].

This platform's tool-changer mechanism applies principles of exact constraint design and Maxwell's criterion. An equilateral triangle layout of a Maxwell-style interface is used, as its symmetry facilitates manufacturing while still providing repeatability. A base plate was modeled using SOLIDWORKS with the three characteristic V-grooves, while a toolhead plate was designed with complementary spherical components. This base plate mounts to the Cartesian

robot, while the toolhead plate is stored on a tool rack for automatic coupling when needed during the test process. All custom-made components are manufactured out of 17-4PH Stainless Steel using metal fused filament fabrication for increased strength.

Calculations were made using equilibrium equations based on Newton's laws of motion to approximate a minimum preload requirement for this application. Assuming a single spring is used to provide the preload, the minimum preload force was determined to be

$$F_{s,min} = 0.409 \cdot W_t + 10.9 \text{ N},$$

where W_t is the weight of the toolhead. Considering the toolhead weight to be negligible, the minimum preload was determined to be approximately 10.9 Newtons.

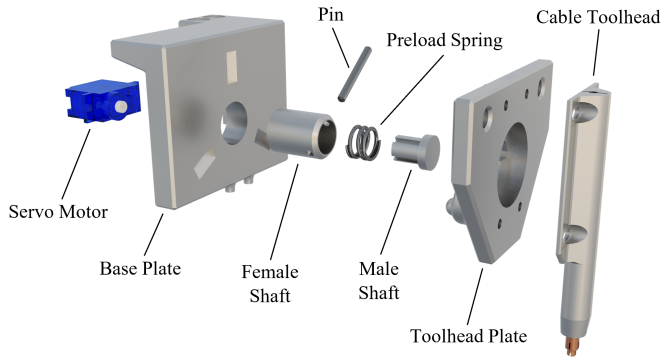

Figure 8: Tool-Changer Exploded View

An actuatable mechanism was created to apply a preload force when toolhead use is desired. A factor of safety of 4 was chosen for this force to guarantee platform support of future tools. The components of this mechanism are shown in Figure 8. A 23.3 Newton per millimeter spring with a free length of 7.72 millimeters was selected for this application. These mechanical properties ensure that the minimum preload of 10.9 Newtons can be readily achieved with a compact design.

During assembly, the spring and male shaft are placed inside the female shaft such that a force is generated by pulling the two shafts apart. To generate this pulling motion, the pin is rotated to travel up a circular inclined ramp located within the toolhead plate. The height of this ramp is equal to the compression distance of the spring. Therefore, with a maximum height of 2 millimeters, the maximum preload force is 46.6 Newtons: approximately four times the calculated minimum preload. Furthermore, the male shaft is bolted to the shaft of the servo motor, allowing the pin to be actuated automatically.

D. Automation

The control system is built around a Raspberry Pi 4 Model B. An HX711 amplifier samples at 10 Hertz and sends sensor values over I2C to an ESP32-WROOM-32 microcontroller. The microcontroller converts these values to the force data and then forwards them over serial to the Raspberry Pi for processing and storing.

Most of the software is written in Python 3.10.12 and utilizes PyQT5, OpenCV, and other built-in libraries to provide a Graphical User Interface (GUI) easily controlled by the operator. Traditional Cartesian motion controls are provided in addition to a scheduler and a data viewer. The scheduler allows specific tasks to be conducted within a given time frame, enabling cyclical testing without operator interference. For remote access, the Raspberry Pi uses Virtual Network Computing (VNC). This grants the ability to execute tasks, manually control the robot, and view data offsite.

The design of the software adheres to IEEE Std. 7001: Autonomous System Transparency Guidelines. This standard ensures the behavior of a given automated system is easy to understand, improving safety and facilitating maintenance [10]. A flowchart of this software is provided below (Figure 9).

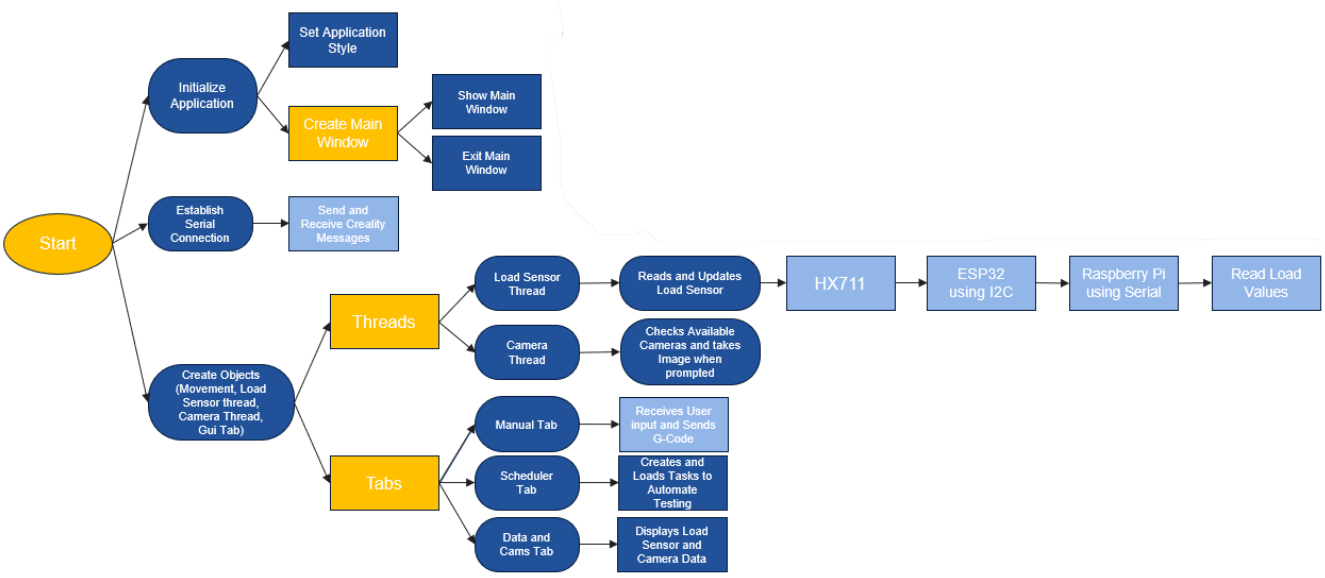

Figure 9: Software Flowchart

IV. Data and Results

Testing the performance of the system occurred in collaboration with Teradyne Inc, who provided the cable fixture and RF cables which are shown in Figure 1. These plugs are approximately 3.5 millimeters in diameter and the tests conducted on the plugs were to determine the change of force during a cable mate.

A force curve of the four mates is shown below (Figure 10). Key areas include the Mate Region, the Transition Region, and the Spring Region as shown in Figure 11. When the male plug begins to enter the female plug, the first interaction between the two is friction from the deformation in the tines on the male plug. This is the Mate Region, which has an observed force rate of approximately 4.29 Newtons per millimeter (downwards). Next, the Transition Region occurs when the male plug reaches the bottom of the female connector without compressing the spring. On average, the slope of this region was 0.06 Newtons per millimeter. The final section of a plug mate force curve is the Spring Region. This occurs when the plug begins compressing the supporting spring after reaching the bottom of the female connector. This observed force rate was 6.13 Newtons per millimeter.

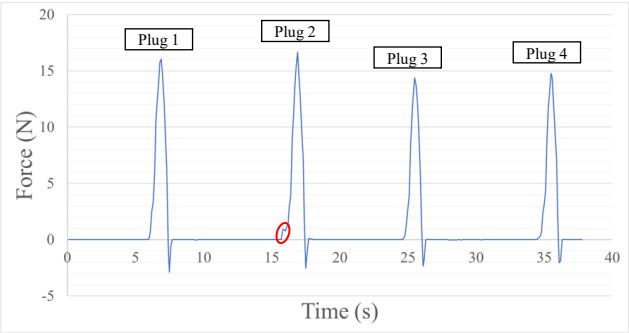

Figure 10: Force Curves of Four Consecutive Mates

These three regions comprise the force profile that is characteristic of these connectors. It is worth noting that the Transition Region is not present in Figure 10; this test collected samples with the male plug plunging at a faster speed and therefore did not capture the Transition Region. An Un-mate Region is also shown in Figure 11, which is the portion of the graph with negative force values (force acting in opposite direction). However, this region is not relevant to fault detection.

This system only has control of the location of the male plug in space–not its orientation. As a result, it cannot account for the compliance in the female plugs. If the male and female connectors are not properly aligned during a mate, they may collide on the edge of the plug. In this event, the force curve illustrates a fault. Within the red zone of Figure 10, the initial force rate of change was approximately 5.33 Newtons per millimeter. This is greater than the 4.29 Newtons per millimeter slope of the Mate Region and closer to the 6.13 Newtons per millimeter force rate of the Spring Region. This shows that linear spring compression is occurring before the Mate Region, which could be used to trigger a halt of the mating process. This is not yet implemented, so the Figure 10 graph reflects the female connector shifting back into position with a small drop in force, before continuing into the Mate Region. Relative to the current state of the art, these results validate this system's improved automation capabilities. In the future, the robot could detect anomalies or account for the compliance in the plugs to avoid them altogether.

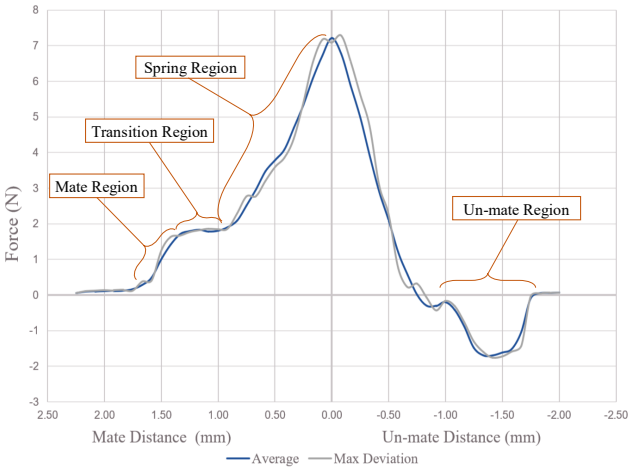

Figure 11: Force Curve with Regions

V. Conclusion

The use of Cartesian robotics and automatic data collection presents a comprehensive improvement to the field of RF machinery testing. This system addresses the challenges posed by delicate RF coaxial connectors through precision automation, force feedback, and remote access capabilities. This is accomplished by combining a Cartesian robot with an automatic tool-changer and incorporating sensor-based imaging and fault detection. The system can ensure mating precision without operator involvement, enhancing test efficiency and reliability. Importantly, the system's adaptable framework, emphasized by its expandable tool-changer, highlights the platform's robust design and scalability.

A. Future Work

While the robot establishes a strong foundation, future work will focus on expanding the system's capabilities by incorporating additional tools that enable a wider range of testing processes. The integration of toolheads such as an RF power analyzer, inspection, and probing toolhead will improve the system's versatility. The inclusion of the power analyzer tool will allow analysis of RF signals during the testing process to provide insight into signal quality and performance. Additionally, an inspection toolhead will ensure damaged cables are identified before a mate is attempted, preventing further harm. To achieve this, images can be taken prior to each action to train a detection algorithm. That same vision system can be expanded to determine the exact location of the plug to compensate for compliance in the connector.

In summary, this project not only accomplishes its primary objectives, but also lays the groundwork for future research and automation in RF machinery testing.

ACKNOWLEDGMENT

This work was supported by Teradyne Inc as well as the H.C. Lord Fund. Thank you to James McCusker and Brian Wadell for their guidance throughout this endeavor.

REFERENCES

[1] M.H. Korayem, A. Iravani, Improvement of 3P and 6R mechanical robots reliability and quality applying FMEA and QFD approaches. Robotics and Computer-Integrated Manufacturing, Volume 24, Issue 3, 2008

[2] J. Frohm, V. Lindström, M. Winroth, & J. Stahre (2006). The industry's view on automation in manufacturing. IFAC Proceedings Volumes, 39(4), 453-458.

[3] T. Thomas, A. Thomas and V. M. Sreekumar, "Design and development of an automated RF test platform for low noise Pre-Amp," 2017 International Conference on Innovative Mechanisms for Industry Applications (ICIMIA), Bengaluru, India, 2017, pp. 177-180, doi: 10.1109/ICIMIA.2017.7975596.

[4] F. Yumbla, J. -S. Yi, M. Abayebas and H. Moon, "Analysis of the mating process of plug-in cable connectors for the cable harness assembly task," *2019 19th International Conference on Control, Automation and Systems (ICCAS)*, Jeju, Korea (South), 2019, pp. 1074-1079, doi: 10.23919/ICCAS47443.2019.8971644.

[5] K. Meredith, "Calculating Mating and Un-mating Forces for Samtec Connectors," Samtec, https://suddendocs.samtec.com/notesandwhitepapers/mating_and_unmating_forces.pdf?CMP=OAD-PUB-CS-samwp-bac618 (accessed Aug. 16, 2023).

[6] J. Huang, P. Di, T. Fukuda and T. Matsuno, "Model-based Robust Online Fault Detection for Mating Process of Electric Connectors in Robotic Wiring Harness Assembly Systems," *2007 International Symposium on Micro-NanoMechatronics and Human Science*, Nagoya, Japan, 2007, pp. 556-563, doi: 10.1109/MHS.2007.4420916.

[7] A. Slocum, "Kinematic Couplings: A Review of Design Principles and Applications." International Journal of Machine Tools and Manufacture 50.4 (2010): 310-327. https://dspace.mit.edu/handle/1721.1/69013.

[8] The principle of kinematic constraint. Practical Precision. (2016, May 16). https://practicalprecision.com/kinematic-constraint/

[9] A. Hart, (2002). Design and Analysis of Kinematic Couplings for Modular Machine and Instrumentation Structures [Master of Science thesis, Massachusetts Institute of Technology].

[10] "IEEE Standard for Transparency of Autonomous Systems," in IEEE Std 7001-2021, vol., no., pp.1-54, 4 March 2022, doi: 10.1109/IEEESTD.2022.9726144.